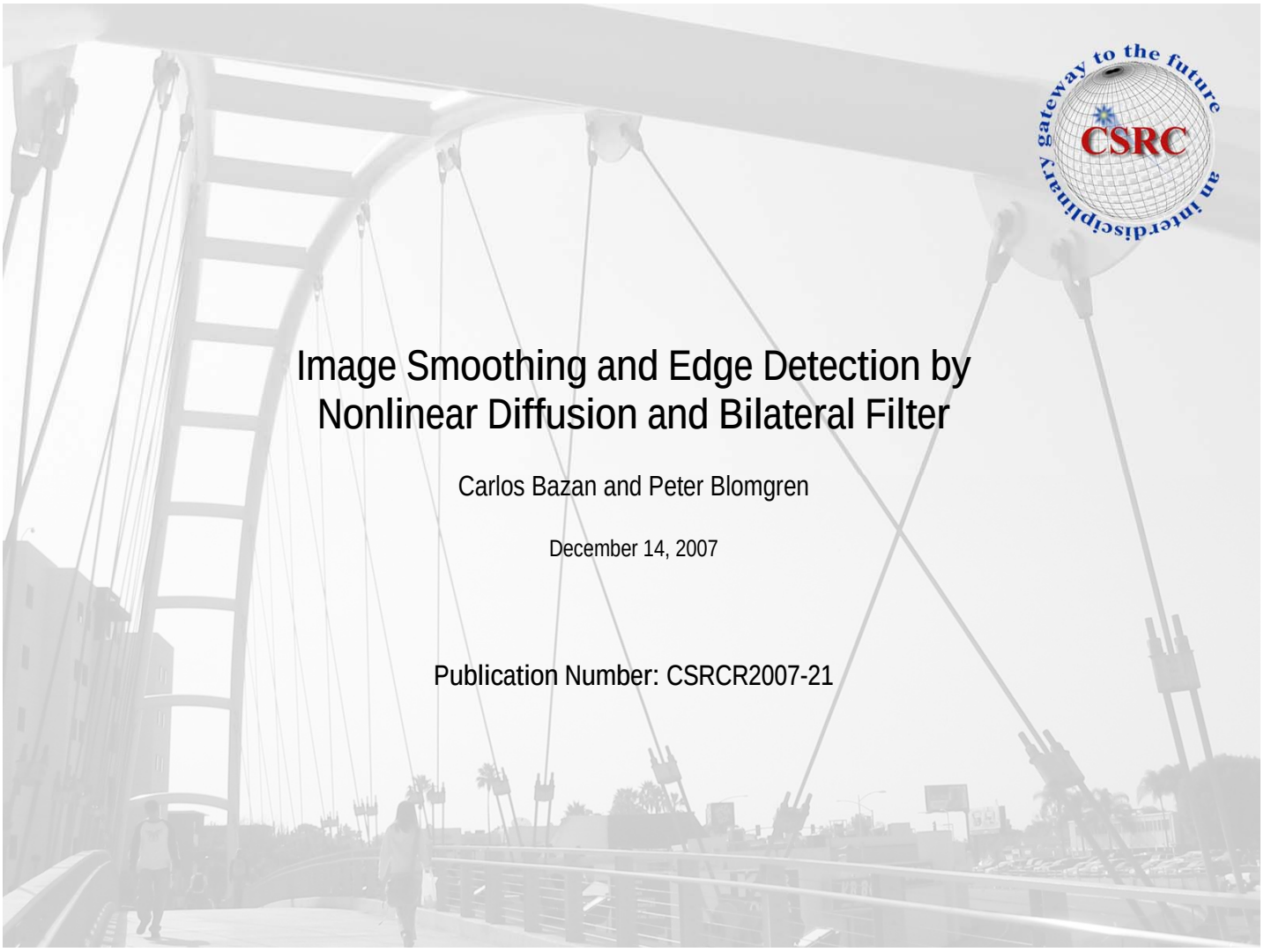

Image Smoothing and Edge Detection by Nonlinear Diffusion and Bilateral Filter

Carlos Bazan and Peter Blomgren

December 14, 2007

Publication Number: CSRCR2007-21

Computational Science & Engineering Faculty and Students Research Articles

Database Powered by the Computational Science Research Center Computing Group & Visualization Lab

COMPUTATIONAL SCIENCE & ENGINEERING

SAN DIEGO STATE UNIVERSITY

Computational Science Research Center
College of Sciences
5500 Campanile Drive
San Diego, CA 92182-1245
(619) 594-3430

Image Smoothing and Edge Detection by Nonlinear Diffusion and Bilateral Filter

Carlos Bazan* and Peter Blomgren†

December 14, 2007

Abstract

In this paper we propose a new image smoothing and edge detection technique that employs a combination of nonlinear diffusion and bilateral filtering. The model is based upon two very well established methodologies in the image processing community, which makes the method easy to understand and implement. Our numerical experiments show that the proposed model is capable of achieving more accurate reconstructions from noisy images, as compared to two other popular nonlinear diffusion models in the literature. We also propose a new and simple diffusion stopping criterion, based on the moving average of the second derivative of the correlation between the noisy image and the filtered image. This indirect measure allows stopping the diffusion process very close to the maximum correlation between the noise-free image and the reconstructed image, in the absence of the former. The stopping criterion is sufficiently general to be applied with most nonlinear diffusion methods normally used for image noise removal.

Keywords: Nonlinear diffusion, bilateral filter, scale-space, image denoising.

AMS subject classification: 35Q80, 68U10.

1 Introduction

Analysis of image features in early vision presents two almost mutually exclusive requirements. On the one hand, it is desirable to smooth homogeneous regions of the image, and on the other hand, we wish to preserve the location of the boundaries or edges accurately. In order to achieve both goals, the classical multiscale analysis theory due to Marr and Hildreth [30], later formalized by Witkin [57], Koenderink [27] and Canny [15], uses a low-pass filtering obtained by convolving the image with Gaussians of increasing variance. Koenderink [27] soon realized that the convolution of the image with a Gaussian at each scale is equivalent to the solution of the heat equation with the image as initial state. Thus, given an image $u_0(\mathbf{x})$, where $\mathbf{x} = (x_1, x_2)$ denotes space coordinates, the scale-space analysis associated with u_0 consists in solving

*Computational Science Research Center, San Diego State University, 5500 Campanile Dr, San Diego, CA 92182-1245, carlos.bazan@sdsu.edu

†Department of Mathematics & Statistics, Dynamical Systems Group & Computational Science Research Center, San Diego State University, 5500 Campanile Dr, San Diego, CA 92182-7720, blomgren@terminus.sdsu.edu

the system[1]

$$\partial_t u - \nabla^2 u = 0, \qquad u(\mathbf{x}, 0) = u_0(\mathbf{x}). \tag{1}$$

This system has a unique solution [49]

$$u(\mathbf{x}, t) = \begin{cases} u_0(\mathbf{x}) & t = 0 \\ \left(G_{\sqrt{2t}} * u_0\right)(\mathbf{x}) & t > 0, \end{cases} \tag{2}$$

provided that (i) the function satisfies $|u(\mathbf{x}, t)| \leq M \exp\left(a |\mathbf{x}|^2\right)$, $M > 0$, (ii) it depends continuously on the initial condition u_0 with respect to $\|\cdot\|_{L^\infty(\mathbb{R}^2)}$, and (iii) it meets the maximum-minimum principle $\inf_{\mathbb{R}^2} u_0 \leqslant u(\mathbf{x}, t) \leqslant \sup_{\mathbb{R}^2} u_0$ on $\mathbb{R}^2 \times [0, \infty)$. The point $\mathbf{x}$ is an edge for the scale t where $|\nabla u(\mathbf{x}, t)|$ is large and $\nabla^2 u(\mathbf{x}, t)$ changes sign.

The simplicity and effectiveness of the Gaussian smoothing makes it an attractive tool for image noise removal. However, it also presents at least a couple of serious drawbacks: (i) Gaussian smoothing does not only smooth the noise but it also smoothes everything else along with it; and (ii) Gaussian smoothing tends to dislocate edges when one moves from a finer to a coarser scale [57, 58]. Most of the shortcomings of linear diffusion processes can be avoided through nonlinear diffusion models.

This paper is organized as follows: In section 2, we describe briefly the nonlinear diffusion models applied in image processing for the reduction of noise and the detection of edges. This serves as background for our proposed model. In section 3, we define our new model for image smoothing and edge detection and conjecture the reasons for its practical success. In section 4, we present some computational examples of the performance of the new model as compared to two other popular models in the literature. In section 5, we propose a simple, yet efficient diffusion stopping criterion for achieving good results when nonlinear diffusion processes are applied. We conclude the paper in section 6 with a discussion and outline of possible future improvements and analysis of the model.

2 Nonlinear Diffusion Models

One of the first attempts to derive a model that incorporates (current) local information from an image within a PDE framework was conducted by Perona and Malik [38]. They proposed a nonlinear diffusion model (which they called 'anisotropic') in order to avoid the blurring of edges and other localization problems

[1] Unless stated otherwise, $\nabla\cdot$ and $\nabla^2\cdot$ involve derivatives with respect to the spatial variable $\mathbf{x}$.

presented by linear diffusion models. The model accomplishes this by applying a process that reduces the diffusivity in places having higher likelihood of being edges. This likelihood is measured by a function of the (current) local gradient $\|\nabla u\|$. The model can be written as

$$\partial_t u - \nabla \cdot \left(g\left(\|\nabla u\|^2 \right) \nabla u \right) = 0, \qquad \partial_{\mathbf{n}} u = 0, \qquad u\left(\mathbf{x}, 0\right) = u_0\left(\mathbf{x}\right), \tag{3}$$

where $\partial_{\mathbf{n}} u = 0$ denotes homogeneous Neumann boundary conditions. In this model the diffusivity has to be such that $g\left(\|\nabla u\|^2 \right) \to 0$ when $\|\nabla u\| \to \infty$ and $g\left(\|\nabla u\|^2 \right) \to 1$ when $\|\nabla u\| \to 0$. One of the diffusivities Perona and Malik proposed is

$$g\left(\|\nabla u\|^2 \right) = \frac{1}{1 + \|\nabla u\|^2 \Big/ \lambda^2}, \qquad \lambda > 0, \tag{4}$$

where λ is a threshold (contrast) parameter that separates forward and backward diffusion [49]. The model accomplishes the long sought effect of blurring small fluctuations (possible noise) while enhancing edges. The results obtained by Perona and Malik are visually very impressive.

Notwithstanding the practical success of the Perona-Malik model, it presents some serious theoretical problems: (i) None of the classical well-posedness frameworks is applicable to the Perona-Malik model, *i.e.* we can not ensure well-posedness results [53, 34]; (ii) Uniqueness and stability with respect to the initial image should not be expected, *i.e.* solvability is a difficult problem, in general [26, 25, 24, 39, 16]; (iii) The regularizing effect of the discretization plays too much of an important role in the solution [23, 9]. The latter is perhaps the key element in the success or failure of the model. Most practical applications work very well provided that the numerical schemes stabilize the process through some implicit regularization.

This observation motivated much research towards the introduction of the regularization directly into the PDE to avoid the dependence on the numerical schemes [16, 34]. A variety of spatial, spatio-temporal, and temporal regularization procedures have been proposed over the years [8, 16, 51, 49, 55, 28]. The one that has attracted much attention is the mathematically sound formulation due to Catté, Lions, Morel and Coll [16]. They proposed replacing the diffusivity $g\left(\|\nabla u\|^2 \right)$ of the Perona-Malik model by a slight variation $g\left(\|\nabla u_\sigma\|^2 \right)$ with $u_\sigma = G_\sigma * u$, where G_σ is a smooth kernel (Gaussian of variance σ^2). Their proposed model is therefore

$$\partial_t u - \nabla \cdot \left(g\left(\|\nabla u_\sigma\|^2 \right) \nabla u \right) = 0, \qquad \partial_{\mathbf{n}} u = 0, \qquad u\left(\mathbf{x}, 0\right) = u_0\left(\mathbf{x}\right). \tag{5}$$

We should note that this spatial regularization model belongs to a class of well-posed problems (existence and uniqueness were proven in [16]), and that its successful implementation is contingent on the choosing of an appropriate value for the additional regularization parameter σ. Whitaker and Pizer [55] and Li and Chen [28] suggested making the parameters σ and λ time-dependent, and Benhamouda [9] performed a systematic study of the influence of these parameters for the one-dimensional case.

Another interesting variation to the Perona-Malik model is the one proposed by Alvarez, Lions and Morel [2]. They refined (5) further and proposed and studied a class of nonlinear parabolic differential equations of the form

$$\partial_t u - g\left(|G * \nabla u|\right) |\nabla u| \, \nabla \cdot \left(\frac{\nabla u}{|\nabla u|} \right) = 0, \qquad \partial_{\mathbf{n}} u = 0, \qquad u\left(\mathbf{x}, 0\right) = u_0\left(\mathbf{x}\right). \tag{6}$$

The degenerate diffusion term $|\nabla u| \, \nabla \cdot (\nabla u / |\nabla u|)$ diffuses u in the direction orthogonal to its gradient ∇u and prevents diffusion in the direction of ∇u. The term $g\left(|G * \nabla u|\right)$ is used for edge enhancement and it controls the speed of the diffusion.

3 Nonlinear Diffusion and Bilateral Filtering

In the Catté-Lions-Morel-Coll model the term inside the divergence, $g\left(\|\nabla u_\sigma\|^2\right)$, is a function of the gradient of the solution at scale σ of the heat equation with $u\left(\mathbf{x}, 0\right)$ as initial state. Consequently, it is equivalent to using an estimate of the gradient of u at point $\mathbf{x}$, obtained by the classical theory [2]. In practice, after the Gaussian (domain) filtering is performed, the term $g\left(\|\nabla u_\sigma\|^2\right)$ allows detection of the locations of the main edges and prevents excessive diffusion at these locations. By the same token, the small fluctuations (noise) will be smooth enough (avoiding them being mistaken for edges) and can be diffused away.

In this paper we propose using a refined estimate of the gradient of u at point $\mathbf{x}$, obtained by applying a bilateral filter in place of the Gaussian kernel. Bilateral filtering is a technique for smoothing images while preserving edges. The first application of this method is attributed to Aurich and Weule [3], and it was subsequently rediscovered by Smith and Brady [43] and Tomasi and Manduchi [46]. Since its introduction, the bilateral filter has been successfully employed in various contexts [10, 1, 29, 35, 19, 40, 20, 22, 5, 42, 56]. Its characteristics and behavior have been the subjects of extensive theoretical studies [44, 47, 48, 21, 6, 7, 19, 13, 33, 36] which have made bilateral filtering a fairly well understood process.

The basic idea underlying bilateral filtering is to combine domain and range filtering, thereby enforcing

both geometric and photometric locality. The model can be expressed as

$$BF\left(u\left(\mathbf{x}\right)\right)=\frac{1}{W\left(\mathbf{x}\right)}\int_{\Omega}G_{\sigma_{s}}\left(\xi,\mathbf{x}\right)G_{\sigma_{r}}\left(u\left(\xi\right),u\left(\mathbf{x}\right)\right)*u\left(\xi\right)d\xi, \tag{7}$$

with the normalization constant

$$W\left(\mathbf{x}\right)=\int_{\Omega}G_{\sigma_{s}}\left(\xi,\mathbf{x}\right)G_{\sigma_{r}}\left(u\left(\xi\right),u\left(\mathbf{x}\right)\right)d\xi. \tag{8}$$

Typically, G_{σ_s} will be a spatial Gaussian that decreases the influence of distant pixels, while G_{σ_r} will be a range Gaussian that decreases the influence of pixels ξ with intensity values that are very different from those of $u\left(\mathbf{x}\right)$, *e.g.*

$$G_{\sigma_{s}}=\exp\left(-\frac{\left|\xi-\mathbf{x}\right|^{2}}{2\sigma_{s}^{2}}\right),\qquad G_{\sigma_{r}}=\exp\left(-\frac{\left|u\left(\xi\right)-u\left(\mathbf{x}\right)\right|^{2}}{2\sigma_{r}^{2}}\right). \tag{9}$$

Parameters σ_s and σ_r dictate the amount of filtering applied in the domain and the range of the image, respectively. This filtering technique, as presented thus far, has the possible objection that it might consist of an expensive proposition. Fortunately, several authors have addressed this limitation and devised very efficient implementations of the method [41, 54, 36, 17]. In our application, we use the fast approximation due to Paris and Durand [36] which employs downsampling in the domain and range that achieves important acceleration of the bilateral filtering.

The proposed model is therefore

$$\partial_{t}u-\nabla\cdot\left(g\left(\left\|\nabla u_{BF}\right\|^{2}\right)\nabla u\right)=0,\qquad\partial_{\mathbf{n}}u=0,\qquad u\left(\mathbf{x},0\right)=u_{0}\left(\mathbf{x}\right). \tag{10}$$

Where $u_{BF}=BF\left(u\left(\mathbf{x}\right)\right)$ is the domain- and range-filtered image (7), and $g\left(s\right)$ is a smooth nonincreasing function with $g\left(0\right)=1$, $g\left(s\right)\geqslant 0$, and $g\left(s\right)$ tending to zero at infinity. We should recall here that the main purpose of the function $g\left(s\right)$ is to provide 'intelligent' smoothing. It should not only inhibit diffusion at edges and allow it far from them, but it should also precisely locate the position of the main edges. By design, this is exactly what bilateral filtering accomplishes. It provides image smoothing with strict preservation of the edges without artificially enhancing them.

The practical success of the proposed model has one its roots in the connection that exists between bilateral filtering and the Perona-Malik-based methods. Buades, Coll and Morel [14] have established the

link existing between bilateral filtering and well-known PDE models such as the heat equation and the Perona-Malik equation. They have proven that for small neighborhoods, bilateral filtering using a box function as spatial weight, asymptotically behaves as the Perona-Malik model. In a discrete setting, Durand and Dorsey [19] have shown that the bilateral filter, if constrained to the four neighbors of each pixel, corresponds to a discrete version of the Perona-Malik filter. Subsequently, Barash [6] used adaptive smoothing as a link between anisotropic diffusion and bilateral filtering, each of which can be viewed as a generalization of the former; while Elad [21] and Barash and Comaniciu [7] have shown that bilateral filtering is equivalent to a sum of several Perona-Malik filters at different scales.

4 Numerical Experiments

In order to compare the performance of the proposed model we implemented the three models below using finite difference, and a simple performance measure based on the correlation between the noise-free image and the three filtered images. Model 1 is the classic Perona-Malik model (3)

$$\begin{aligned} &\partial_t u - \nabla \cdot \left(g\left(\|\nabla u\|^2 \right) \nabla u \right) = 0, \qquad \partial_{\mathbf{n}} u = 0, \qquad u\left(\mathbf{x}, 0\right) = u_0\left(\mathbf{x}\right), \\ &g\left(\|\nabla u\|^2 \right) = \frac{1}{1 + \|\nabla u\|^2 \Big/ \lambda^2}, \qquad \lambda = 10^{-2}. \end{aligned} \tag{11}$$

Parameter $\lambda = 10^{-2}$ was estimated as an average of the 'robust scale' proposed in [11, 12], using the initial state of the images employed in our tests. Model 2 is the Perona-Malik variant by Catté, Lions, Morel and Coll (5)

$$\begin{aligned} &\partial_t u - \nabla \cdot \left(g\left(\|\nabla u_\sigma\|^2 \right) \nabla u \right) = 0, \qquad \partial_{\mathbf{n}} u = 0, \qquad u\left(\mathbf{x}, 0\right) = u_0\left(\mathbf{x}\right), \\ &g\left(\|\nabla u\|^2 \right) = \frac{1}{1 + \|\nabla u_\sigma\|^2 \Big/ \lambda^2}, \qquad \lambda = 10^{-2}, \\ &u_\sigma = G_\sigma * u, \qquad \sigma = 1. \end{aligned} \tag{12}$$

It has been shown [31] that $\sigma = 1$ is sufficient for a large interval of noise variances provided that the noise in neighboring pixels is uncorrelated and that the grid size is one. Model 3 is the proposed model (10)

$$
\begin{aligned}
&\partial_t u - \nabla \cdot \left(g\left(\left\| \nabla u_{BF} \right\|^2 \right) \nabla u \right) = 0, \qquad \partial_{\mathbf{n}} u = 0, \qquad u\left(\mathbf{x}, 0\right) = u_0\left(\mathbf{x}\right), \\
&g\left(\left\| \nabla u \right\|^2 \right) = \frac{1}{1 + \left\| \nabla u_{BF} \right\|^2 \Big/ \lambda^2}, \qquad \lambda = 10^{-2}, \\
&u_{BF} = BF\left(u\right), \qquad \sigma_s = 3, \;\; \sigma_r = 10^{-2}.
\end{aligned}
\tag{13}
$$

The parameters σ_s and σ_r are chosen according to the desired amount of low-pass filtering and desired amount of combination of pixel values, respectively [46]. We loosely followed the recommendations given in [29] for choosing σ_s, and the ones in [37] for choosing σ_r. They give us a compact kernel that allows a very fast execution of the bilateral filtering.

The experiment consisted in running the three models using an explicit Euler method with a time step[2] of $\delta t = 10^{-2}$, and trying to restore the noise-free image, $f\left(\mathbf{x}\right)$, that has been perturbed by additive Gaussian white noise. The three models were run for 50 iterations and the correlation coefficient between the noise-free image and each of the filtered images was measured at each iteration. For every case, we observe that the best image reconstructed by the proposed model is closer to the noise-free image than the best images reconstructed by the other two models tested (see Fig. 1, 2 and 3). We can also observe that the proposed model performs 'in between' the other two models in terms of speed of reconstruction. The Catté-Lions-Morel-Coll model accomplishes the fastest reconstruction, *i.e.* it attains its best reconstructed image in fewer iterations than the other two methods. The classic Perona-Malik model achieves a better reconstruction if one were to iterate beyond the optimal stopping times of the three models, *i.e.* 50 iterations in this case. Lastly, in order for any of the three models to accomplish its best possible reconstruction, one has to be able to stop the diffusion process at the peak of its performance, in the absence of the noise-free image. In general, this remains an open problem. In the next section we propose a procedure that works very well all the models considered in this paper.

5 Diffusion Stopping Criterion

Determining when the diffusion process should be stopped is crucial for obtaining a good image reconstruction. Several authors have addressed this issue in the past in an attempt to devise an optimal stopping criterion. Sporring and Weickert [45] focused on the maximal entropy change by scale to estimate the size of image structures. They argued that the minimal change by scale indicates especially stable scales with

[2] Weickert [52] has shown that, for explicit discretization schemes, the stability condition (assuming $\delta\mathbf{x} = 1$ and $\forall s : g\left(s\right) \leqslant 1$) is $\delta t < 1/(2d)$, with d being the number of dimensions of the data, which for a 2D image $d = 2$.

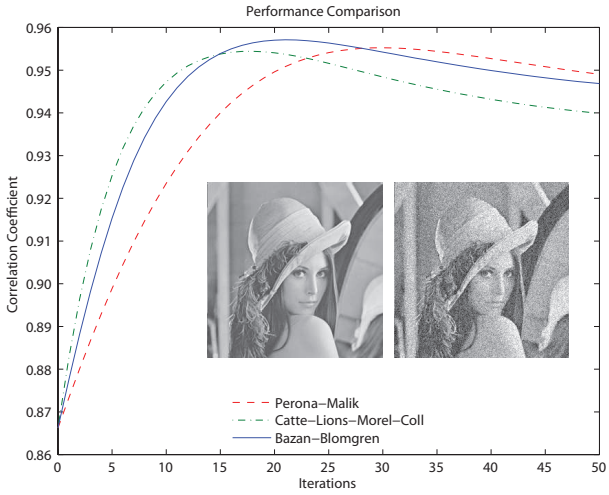

Figure 1: Correlation coefficient between the noise-free image of Lena and the filtered image of Lena at each iteration, along with the noise-free image of Lena (left) and the noisy image of Lena (right) corrupted by additive Gaussian white noise, $SNR = 17.4$ dB. The maximum value of the correlation coefficient for each model is as follows: Perona-Malik, 0.9553; Catté-Lions-Morel-Coll, 0.9544; Bazan-Blomgren, 0.9571.

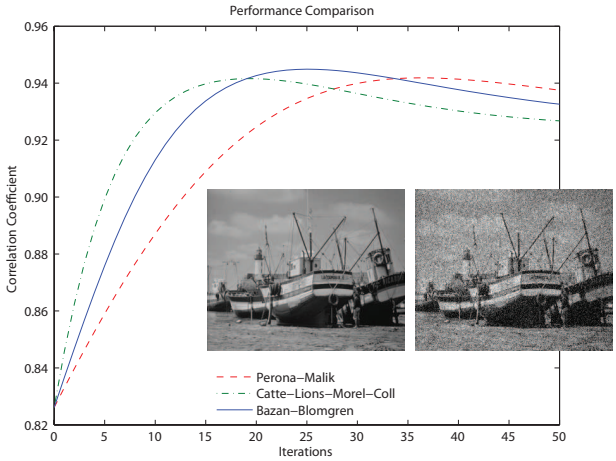

Figure 2: Correlation coefficient between the noise-free image of the Boats and the filtered image of the Boats at each iteration, along with the noise-free image of the Boats (left) and the noisy image of the Boats (right) corrupted by additive Gaussian white noise, $SNR = 18.9$ dB. The maximum value of the correlation coefficient for each model is as follows: Perona-Malik, 0.9418; Catté-Lions-Morel-Coll, 0.9416; Bazan-Blomgren, 0.9449

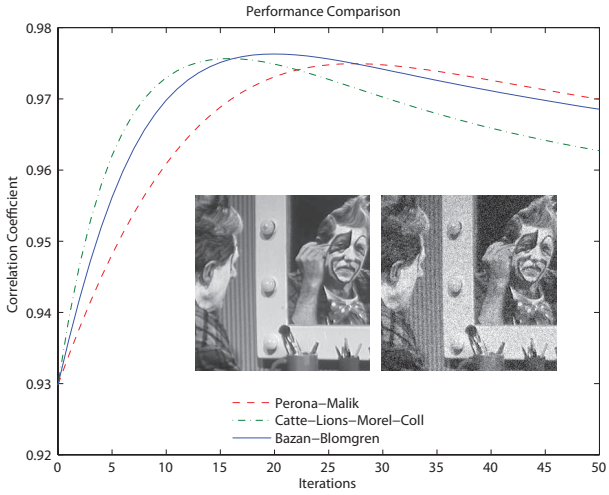

Figure 3: Correlation coefficient between the noise-free image of the Clown and the filtered image of the Clown at each iteration, along with the noise-free image of the Clown (left) and the noisy image of the Clown (right) corrupted by additive Gaussian white noise, $SNR = 21.2$ dB. The maximum value of the correlation coefficient for each model is as follows: Perona-Malik, 0.9749; Catté-Lions-Morel-Coll, 0.9757; Bazan-Blomgren, 0.9763.

respect to evolution time, and conjectured that these scales could be good candidates for stopping times in nonlinear diffusion processes. Weickert [50] also pointed out that the monotonically decreasing 'relative variance', $0 \leqslant \mathrm{var}\,(u)/\mathrm{var}\,(u_0) \leqslant 1$, could be used to measure the distance of u from the initial state u_0 and, by prescribing an appropriate value for the relative variance, it can constitute a good criterion for stopping the nonlinear diffusion.

Dolcetta and Ferretti [18] formulated a stopping criterion within the framework of optimal control theory. They considered the minimization of the performance index

$$E\,(t) = \int_0^t (E_c + E_\alpha)\,dt, \tag{14}$$

where E_c is the computing cost and E_α is the stopping cost, which encourages diffusion for small values of the scale factor. The authors argued that a careful balancing of the two terms is necessary for achieving good results, and suggested to take $E_c = c$ and $E_\alpha = -\left(\int_\Omega |u - u_0|^2\,dx\right)^{\frac{\alpha}{2}}$, for some positive constants c and α. Mrázek [32] developed a new interesting time-selection strategy based on the correlation between the signal and the noise. He argued that, if the noise-free image and the noise were uncorrelated, it is appropriate to require that their artificial substitutes u and $(u_0 - u)$ share the same property, and select the stopping time such that $t = \arg\min_t \mathrm{corr}\,(u_0 - u, u)$. The author also pointed out that the assumption about

the noise-free image and the noise being uncorrelated holds initially, but it does not necessarily hold for the filtered image, u, and the filtering noise $(u_0 - u)$. More recently, Awate and Whitaker [4] found empirically that entropy reduction by gradient descent reduces the randomness introduced by the noise faster than it reduces the inherent randomness in the signal. They suggested that an efficient stopping time would be when the relative rate of change of entropy, within two consecutive iterations, falls below some threshold to be chosen.

We propose a new (very simple) diffusion-stopping criterion inspired by observation of the behavior of the correlation between the noise-free image and the filtered image, $\mathrm{corr}\,(f, u)$, and the correlation between the noisy image and the filtered image, $\mathrm{corr}\,(u_0, u)$. Although the former measure is only available in experimental settings it helps validate the usefulness of the latter. The nonlinear diffusion process starts from the observed (noisy) image, $u_0\,(\mathbf{x})$, and creates a set of filtered images, $u\,(\mathbf{x}, t)$, by gradually removing noise and details from scale to scale until, as $t \to \infty$, the image converges to a constant value. During this process the correlation between the noise-free image and the filtered image increases as the filtered image moves closer to the noise-free image. This behavior continues until it reaches a peak from where the measure decreases as the filtered image moves slowly towards a constant value. During the same process the correlation between the noisy image and the filtered image decreases gradually from a value of 1.0 (perfect correlation), to a constant value, $\approx \mathrm{corr}\,(f, u_0)$, as the filtered image becomes smoother (see Fig. 4). By comparing both measures we observe that as $\mathrm{corr}\,(f, u)$ reaches its maximum (best possible reconstructed image), the curvature of $\mathrm{corr}\,(u_0, u)$ changes sign. This suggests that a good stopping point of the diffusion process is where the second derivative of $\mathrm{corr}\,(u_0, u)$ reaches a maximum. In order to avoid 'false positives', we found it is best to 'smooth' the measure of the second derivative, say, by a moving average of the measure[3].

The performance of the proposed stopping criterion can be observed below along with the reconstructed images of 'Lena' (Fig. 5 and 6), the 'Boats' (Fig. 7 and 8), and the 'Clown' (Fig. 9 and 10). We observe that the stopping criterion is almost optimal, allowing the diffusion process to stop near the point when the three filtering methods reach their best possible image reconstructions. In our experiments, we also observed that the stopping criterion overestimate or underestimate the stopping time under two circumstances: when the noisy image has excess details, *e.g.* the 'Baboon' (see Fig. 11-left), the stopping criterion tends to stop a little too late, causing some lost of details (this phenomenon has been also observed in [31].) When the noisy image is cartoon-like image, *e.g.* the 'Cameraman' (see Fig. 11-right), the stopping criterion tends to stop a little too soon, causing a premature output. This is due to the design of the filters which prevent

[3]In our experiments we used an exponential moving average of width 4.

diffusion across edges.

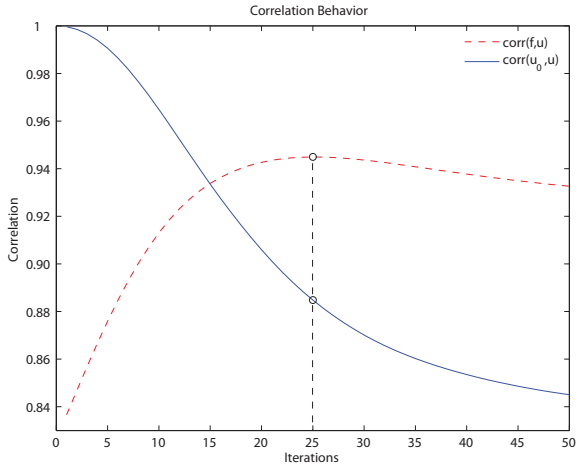

Figure 4: The correlation coefficient between the noise-free image and the filtered image increases as the filtered image moves closer to the noise-free image. When the measure reaches a peak it decreases as the filtered image moves slowly towards a constant value. The correlation coefficient between the noisy image and the filtered image decreases gradually from a value of 1.0 (perfect correlation), to a constant value as the filtered image becomes smoother.

6 Discussion

In this paper we propose a new image smoothing and edge detection technique by combining two very well established methods based on nonlinear diffusion and bilateral filtering. The new model is able to obtained the best possible reconstruction of a noisy image as measured by the correlation coefficient between the noise-free image and the reconstructed image. In a real-world situation, the true (unperturbed) image would not be known, hence the correlation coefficient between this and the reconstructed image could not be measured. Therefore, we also propose a new and simple diffusion stopping criterion, based on the moving average of the second derivative of the correlation between the noisy image and the filtered image. This measure allows one to stop the diffusion process close to the point of maximum similarity between the noise-free image and the filtered image. Furthermore, no knowledge (e.g. noise variance, noise and signal correlation or lack-off, etc.) is required to implement the stopping criterion, which makes the method applicable under a wide range of noise conditions. Some further research has to also be done to make the stopping criterion suitable for the two exception cases mentioned above. Also, more rigorous analytical analysis should be made for a better understanding of the successful practical performance of the proposed model.

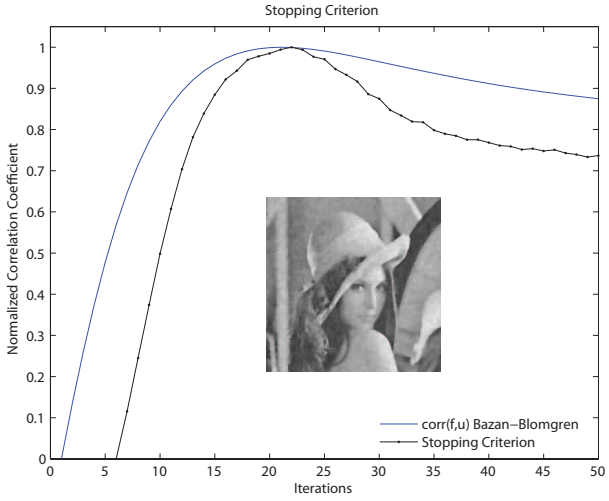

Figure 5: Stopping criterion performance along with the reconstructed image of Lena using the proposed model. The measure corr (f, u) suggests stopping the diffusion process after 21 iterations, while the proposed stopping criterion suggests to stop the diffusion process after 22 iterations.

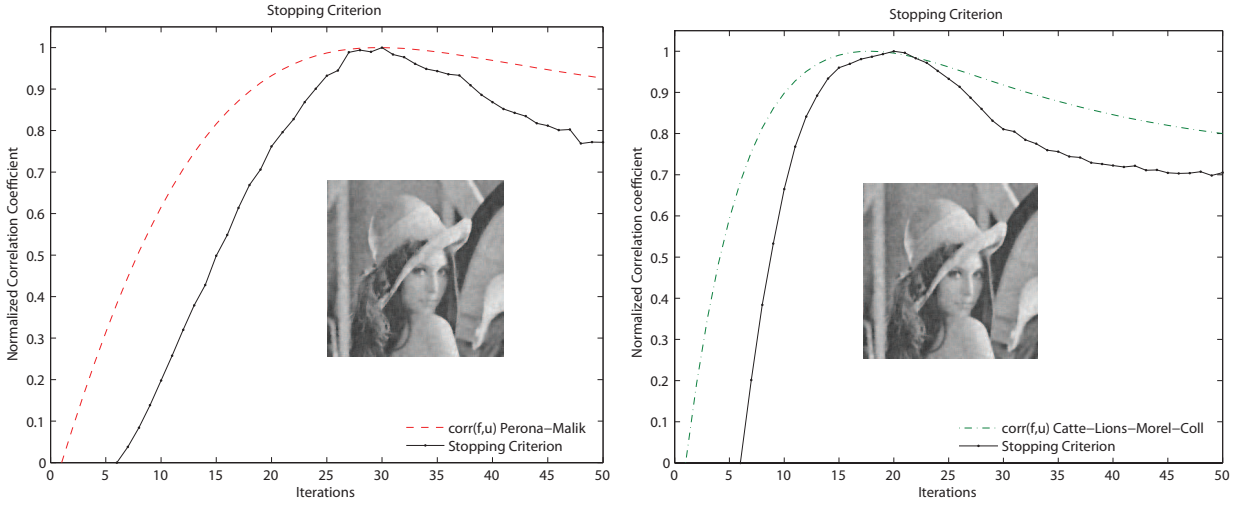

Figure 6: (left) Stopping criterion performance along with the reconstructed image of Lena using the Perona-Malik model. The measure corr (f, u) suggests stopping the diffusion process after 30 iterations, while the proposed stopping criterion suggests to stop the diffusion process after 28 iterations. (right) Stopping criterion performance along with the reconstructed image of Lena using the Catté-Lions-Morel-Coll model. The measure corr (f, u) suggests stopping the diffusion process after 18 iterations, while the proposed stopping criterion suggests to stop the diffusion process after 20 iterations.

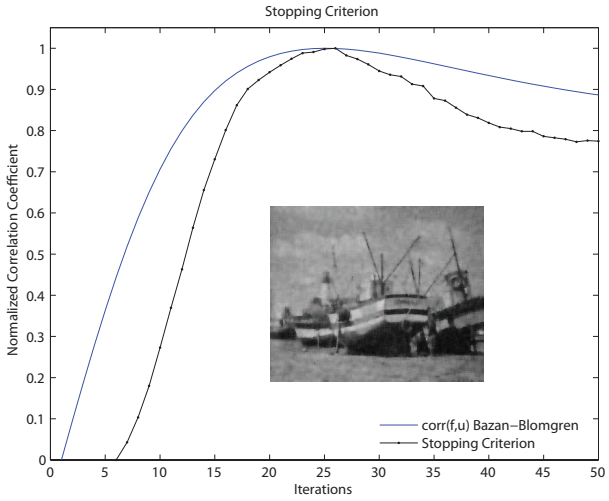

Figure 7: Stopping criterion performance along with the reconstructed image of the boats using the proposed model. The measure corr (f, u) suggests stopping the diffusion process after 25 iterations, while the proposed stopping criterion suggests to stop the diffusion process after 26 iterations.

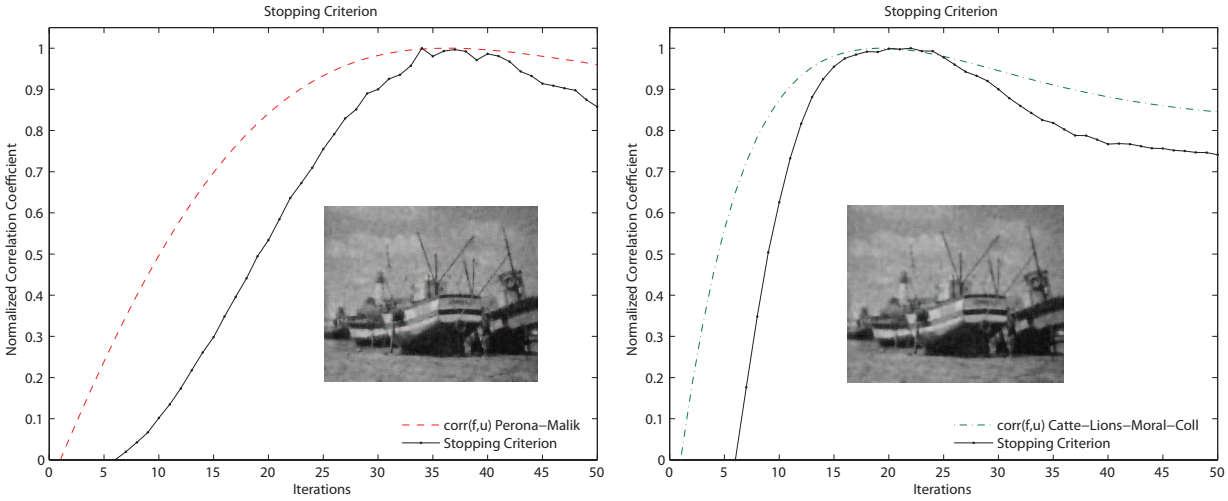

Figure 8: (left) Stopping criterion performance along with the reconstructed image of the boats using the Perona-Malik model. The measure corr (f, u) suggests stopping the diffusion process after 36 iterations, while the proposed stopping criterion suggests to stop the diffusion process after 34 iterations. (right) Stopping criterion performance along with the reconstructed image of the boats using the Catté-Lions-Morel-Coll model. The measure corr (f, u) suggests stopping the diffusion process after 19 iterations, while the proposed stopping criterion suggests to stop the diffusion process after 22 iterations.

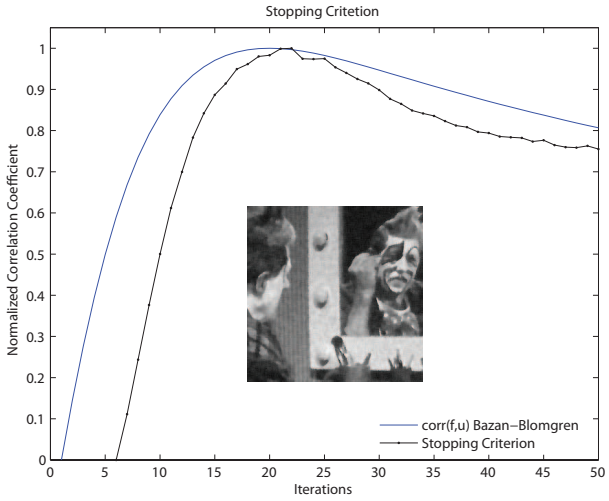

Figure 9: Stopping criterion performance along with the reconstructed image of the Clown using the proposed model. The measure corr (f, u) suggests stopping the diffusion process after 20 iterations, while the proposed stopping criterion suggests to stop the diffusion process after 22 iterations.

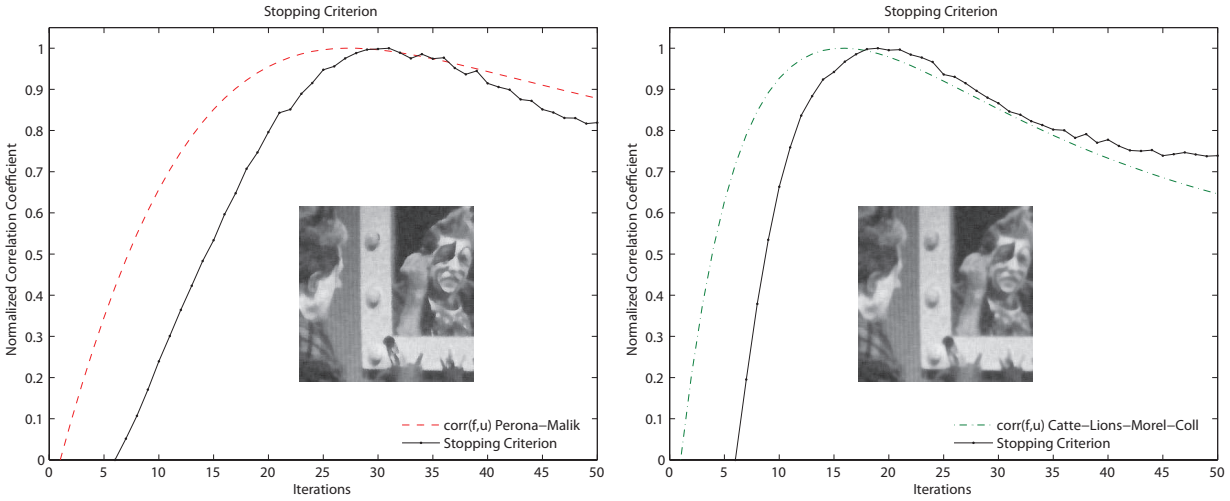

Figure 10: (left) Stopping criterion performance along with the reconstructed image of the Clown using the Perona-Malik model. The measure corr (f, u) suggests stopping the diffusion process after 27 iterations, while the proposed stopping criterion suggests to stop the diffusion process after 31 iterations. (right) Stopping criterion performance along with the reconstructed image of the Clown using the Catté-Lions-Morel-Coll model. The measure corr (f, u) suggests stopping the diffusion process after 16 iterations, while the proposed stopping criterion suggests to stop the diffusion process after 19 iterations.

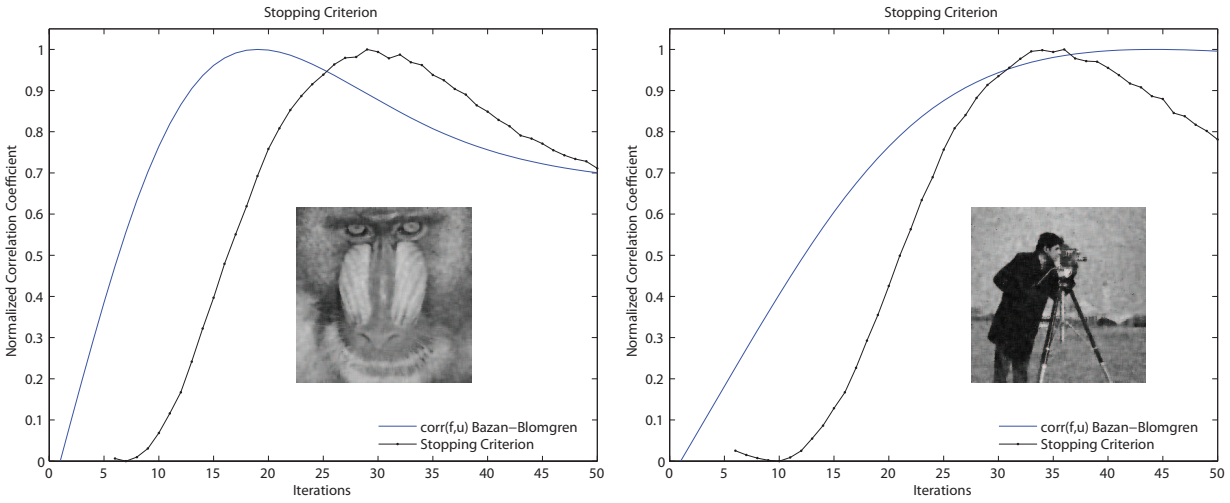

Figure 11: (left) Stopping criterion performance along with the reconstructed image of the Baboon using the proposed model. The measure corr (f, u) suggests stopping the diffusion process after 19 iterations, while the proposed stopping criterion suggests to stop the diffusion process after 29 iterations. (right) Stopping criterion performance along with the reconstructed image of the Cameraman using the proposed model. The measure corr (f, u) suggests stopping the diffusion process after 44 iterations, while the proposed stopping criterion suggests to stop the diffusion process after 34 iterations.

7 Acknowledgments

This work has been supported in part by NIH RoadMap Initiative award R90 DK07015.

References

[1] M. Aleksic, M. Smirnov, and S. Goma. Novel bilateral filter approach: Image noise reduction with sharpening. In *Proceeding of the Digital Photography II Conference*, pages 141–147. SPIE, 2006.

[2] L. Alvarez, P.-L. Lions, and J.-M. Morel. Image selective smoothing and edge detection by nonlinear diffusion, II. *SIAM Journal on Numerical Analysis*, 29(3):845–866, 1992.

[3] V. Aurich and J. Weule. Non-linear gaussian filters performing edge preserving diffusion. In *Proceedings of the DAGM Symposium*, volume 17, pages 538–545. Deutsche Arbeitsgemeinschaft für Mustererkennung, 1995.

[4] S. Awate and R. Whitaker. Unsupervised, information-theoretic, adaptive image filtering for image restoration. *IEEE Transactions on Pattern Analysis and Machine Intelligence*, 28(3):364–376, 2006.

[5] S. Bae, S. Paris, and F. Durand. Two-scale tone management for photographic look. *ACM Transactions on Graphics*, 25(3):637–645, 2006.

[6] D. Barash. A fundamental relationship between bilateral filtering, adaptive smoothing and nonlinear diffusion equation. *IEEE Transactions on Pattern Analysis and Machine Intelligence*, 24(6):844–847, 2002.

[7] D. Barash and D. Comaniciu. A common framework for nonlinear diffusion, adaptive smoothing, bilateral filtering and mean shift. *Image and Video Computing*, 22(1):73–81, 2004.

[8] G.I. Barenblatt, M. Bertsch, R. Dal Passo, and M. Ughi. A degenerate pseudo-parabolic regularization of a nonlinear forward-backward heat equation arising in the theory of heat and mass exchange in stably stratified turbulent shear flow. *SIAM Journal on Mathematical Analysis*, 24(6):1414–1439, 1993.

[9] B. Benhamouda. Parameter adaptation for nonlinear diffusion in image processing. Master's thesis, University of Kaiserslautern, Kaiserslautern, 1994.

[10] E.P. Bennet and L. McMillan. Video enhancement using per-pixel virtual exposures. *ACM Transactions on Graphics*, 24(3):845–852, 2005.

[11] M.J. Black and G. Sapiro. Edges as outliers: Anisotropic smoothing using local image statistics. In M. Nielsen, P. Johansen, O.F. Olsen, and J. Weickert, editors, *Lecture Notes in Computer Science*, number 1682, pages 259–270. Springer, Berlin, Germany, 1999.

[12] M.J. Black, G. Sapiro, D. Marimont, and D. Heeger. Robust anisotropic diffusion. *IEEE Transactions on Image Processing*, 7(3):421–432, 1998.

[13] A. Buades, B. Coll, and J.-M. Morel. Neighborhood filters and PDE's. *Numerische Mathematik*, 105(1):1–34, 2006.

[14] A. Buades, B. Coll, and J.-M. Morel. The staircasing effect in neighborhood filters and its solution. *IEEE Transactions on Image Processing*, 15(6):1499–1505, 2006.

[15] A. Canny. A computational approach to edge detection. *IEEE Transactions on Pattern Analysis and Machine Intelligence*, 8:769–698, 1986.

[16] F. Catté, P.-L. Lions, J.-M. Morel, and T. Coll. Image selective smoothing and edge detection by nonlinear diffusion. *SIAM Journal of Numerical Analysis*, 29(1):182–193, 1992.

[17] J. Chen, S. Paris, and F. Durand. Real-time edge-aware image processing with bilateral grid. *ACM Transactions on Graphics*, 26(3):Article No. 103, 2007.

[18] C. Dolcetta and I. Ferretti. Optimal stopping time formulation of adaptive image filtering. *Applied Mathematics and Optimization*, 43(3):245–258, 2001.

[19] F. Durand and J. Dorsey. Fast bilateral filtering for the display of high-dynamic-range images. *ACM Transactions on Graphics*, 21(3):257–266, 2002.

[20] E. Eisemann and F. Durand. Flash photography enhancement via intrinsic relighting. *ACM Transactions on Graphics*, 23(3):673–678, 2004.

[21] M. Elad. On the bilateral filter and ways to improve it. *IEEE Transactions on Image Processing*, 11(10):1141–1151, 2002.

[22] M. Elad. Retinex by two bilateral filters. *Lecture Notes in Computer Science*, 3459:217–229, 2005.

[23] J. Fröhlich and J. Weickert. Image processing using a wavelet algorithm for nonlinear diffusion. Report 104, Laboratory of Technomathematics, University of Kaiserslautern, Kaiserslautern, 1994.

[24] K. Höllig. Existence of infinitely many solutions for a forward-backward heat equation. *Transactions of the American Mathematical Society*, 278:299–319, 1983.

[25] K. Höllig and J.A. Nohel. A diffusion equation with a non-monotone constitutive function. In J.M. Ball, editor, *Proceedings of NATO/London Mathematical Society Conference on Systems of Partial Differential Equation*, pages 409–422, 1983.

[26] S. Kichenassamy. The perona-malik paradox. *SIAM Journal of Applied Mathematics*, 57(5):1328–1342, 1997.

[27] J.J. Koenderink. The structure of images. *Biological Cybernetics*, 50:363–370, 1984.

[28] X. Li and T. Chen. Nonlinear diffusion with multiple edginess thresholds. *Pattern Recognition*, 27(8):1029–1037, 1994.

[29] C. Liu, W.T. Freeman, R. Szeliski, and S. Kang. Noise estimation from a single image. In *Proceedings of the IEEE Computer Society Conference on Computer Vision and Pattern Recognition*, volume 1, pages 901–908, 2006.

[30] D. Marr and E. Hildreth. Theory of edge detection. In *Proceedings of the Royal Society B*, volume 207, pages 187–217. Royal Society Publishing, 1980.

[31] P. Mrázek. *Nonlinear Diffusion for Image Filtering and Monotonicity Enhancement*. PhD thesis, Czech Technical University, Prague, Czech Republic, 2001.

[32] P. Mrázek. Selection of optimal stopping time for nonlinear diffusion filtering. In M. Kerckhove, editor, *Third International Conference on Scale-Space and Morphology in Computer Vision*, pages 290–298, Berlin, Germany, 2001. IEEE Computer Society, Springer-Verlag.

[33] P. Mrázek, J. Weickert, and A. Bruhn. *On Robust Estimation and Smoothing with Spatial and Tonal Kernels*, pages 335–352. Geometric Properties from Incomplete Data. Springer, Dordrecht, Holland, 2006.

[34] M. Nitzberg and T. Shiota. Nonlinear image filtering with edge and corner enhancement. *IEEE Transactions on Pattern Analysis and Machine Intelligence*, 14(8):826–833, 1992.

[35] B.M. Oh, M. Chen, J. Dorsey, and F. Durand. Image-based modeling and photo editing. In *Proceedings of the International Conference on Computer Graphics and Interactive Techniques*, pages 433–442. ACM, 2001.

[36] S. Paris and F. Durand. A fast approximation of the bilateral filter using a signal processing approach. In *Proceedings of the European Conference on Computer Vision*, pages 568–580, 2006.

[37] S. Paris, P. Kornprobst, and F. Tumblin, J. Durand. A gentle introduction to bilateral filtering and its applications. In *International Conference on Computer Graphics and Interactive Techniques*. ACM SIGGRAPH 2007, Association for Computing Machinery, 2007.

[38] P. Perona and J. Malik. Scale space and edge detection using anisotropic diffusion. *IEEE Transactions on Pattern Analysis and Machine Intelligence*, 12(7):629–639, 1990.

[39] P. Perona, T. Shiota, and J. Malik. Anisotropic diffusion. In B.M. ter Haar Romeny, editor, *Geometry-Driven Diffusion in Computer Vision*, volume 1 of *Computational Imaging and Vision*, pages 72–92. Springer, Kluwer, 1994.

[40] G. Petschnigg, M. Agrawala, H. Hoppe, R. Szeliski, M. Cohen, and K. Toyama. Digital photography with flash and non-flash image pairs. *ACM Transactions on Graphics*, 23(3):664–672, 2004.

[41] T.Q. Pham and L.J. van Vliet. Separable bilateral filtering for fast video preprocessing. In *Proceedings of the IEEE International Conference on Multimedia*, pages 4–7. IEEE, 2005.

[42] R. Ramanath and W.E. Snyder. Adapting demosaicking. *Journal of Electronic Imaging*, 12(4):633–642, 2003.

[43] S.M. Smith and J.M. Brady. SUSAN-a new approach to low level image processing. *International Journal of Computer Vision*, 23(1):45–78, 1997.

[44] N. Sochen, R. Kimmel, and A.M. Bruckstein. Diffusion and confusions in signal and image processing. *Journal of Mathematical Imaging and Vision*, 14(3):237–244, 2001.

[45] J. Sporring and J. Weickert. Information measures in scale-spaces. *IEEE Transactions on Information Theory*, 45(3):1051–1058, 1999.

[46] C. Tomasi and R. Manduchi. Bilateral filtering for gray and color images. In *Proceedings of the IEEE International Conference on Computer Vision*, pages 839–846. IEEE, 1998.

[47] J. van de Weijer and R. van den Boomgaard. Local mode filtering. In *Proceedings of the IEEE Computer Society Conference on Computer Vision and Pattern Recognition*, volume 2, pages 428–433, 2001.

[48] J. van de Weijer and R. van den Boomgaard. On the equivalence of local-mode finding, robust estimation and mean-shift analysis as used in early vision tasks. In *Proceedings of International Conference on Pattern Recognition*, volume 3, pages 927–930, 2002.

[49] J. Weickert. *Anisotropic Diffusion in Image Processing*. PhD thesis, Universität Kaiserslautern, Kaiserslautern, Germany, 1996.

[50] J. Weickert. Coherence-enhancing diffusion of colour images. *Image and Vision Computing*, 17(3):201–212, 1999.

[51] J. Weickert. Efficient image segmentation using partial differential equations and morphology. *Pattern Recognition*, 34(9):1813–1824, 2001.

[52] J. Weickert, B.M.t.H. Romeny, and M.A. Viergever. Efficient and reliable schemes for nonlinear diffusion filtering. *IEEE Transactions on Image Processing*, 7(3):398–410, 1998.

[53] J. Weickert and C. Schnörr. PDE-based preprocessing of medical images. *Kunstliche Intelligenz*, 3:5–10, 2000.

[54] B. Weiss. Fast median and bilateral filtering. *ACM Transactions on Graphics*, 25(3):519–526, 2006.

[55] R.T. Whitaker and S.M. Pizer. A multi-scale approach to non-uniform diffusion. *Computer Vision, Graphics, and Image Processing: Image Understanding*, 57(1):99–110, 1993.

[56] H. Winnermöller, S.C. Olsen, and B. Gooch. Real-time video abstraction. *ACM Transactions on Graphics*, 25(3):1221–1226, 2006.

[57] A.P. Witkin. Space-scale filtering. In A. Bundy, editor, *Proceedings of the Eighth International Joint Conference on Artificial Intelligence*, pages 1019–1022, San Francisco, California, 1983. Morgan Kaufmann.

[58] A.P. Witkin. Scale-space filtering: A new approach to multi-scale description. In *Proceedings of the IEEE International Conference on Acoustic, Speech & Signal Processing*, volume 9, pages 150–153, 1984.